AAPS PharmSciTech, Vol. 16, No. 2, April 2015 (© 2014)
DOI: 10.1208/s12249-014-0218-4

Research Article

Modified Cellulose Nanocrystal for Vitamin C Delivery

Seyedeh Parinaz Akhlaghi,[1] Richard M Berry,[2] and Kam Chiu Tam[1,3]

Received 26 March 2014; accepted 10 September 2014; published online 7 October 2014

Abstract. Cellulose nanocrystal grafted with chitosan oligosaccharide (CNC-CS_{OS}) was used to encapsulate vitamin C and prepare CNCS/VC complexes using tripolyphosphte via ionic complexation. The stability of vitamin C and the antioxidant activity of the CNCS/VC complexes were elucidated. The formation of the complex was confirmed using DSC and UV–vis spectrophotometry, and TEM was used to study the morphology of the complexes. The encapsulation efficiency of vitamin C at pH 3 and 5 was 71.6% ± 6.8 and 91.0 ± 1.0, respectively. Strong exothermic peaks observed in isothermal titration calorimetric (ITC) studies at pH 5 could be attributed to additional electrostatic interactions between CNC-CS_{OS} and vitamin C at pH 5. The *in vitro* release of vitamin C from CNCS/VC complexes showed a sustained release of up to 20 days. The vitamin C released from CNCS/VC complex displayed higher stability compared with the control vitamin C solution, and this was also confirmed from the ITC thermograms. CNC-CS_{OS} possessed a higher scavenging activity and faster antioxidant activity compared with its precursors, i.e., oxidized CNC and CS_{OS} and their physical mixtures. Complexing vitamin C into CNC-CS_{OS} particles yielded a dynamic antioxidant agent, where the vitamin C is released over time and displayed sustained antioxidant properties. Therefore, CNCS/VC can potentially be used in cosmeceutical applications as topical formulations.

KEY WORDS: cellulose nanocrystals; chitosan oligosaccharide; controlled release; vitamin C antioxidant activity.

INTRODUCTION

Antioxidants protect our body from the damage caused by free radicals. Environmental factors such as air pollution, cigarette smoke, and sunlight produce free radicals that damage the skin (1). An effective antioxidant in biological systems is vitamin C (L-ascorbic acid) that serves as a cofactor in hydroxylation reactions and scavenges reactive oxygen species (2). Similar to other important antioxidants, vitamin C is only provided exogenously, therefore, topical application of vitamin C is beneficial as a protector for the skin (3).

Vitamin C has also been used in different cosmetic and pharmaceutical formulations because of its beneficial effects on the skin (4,5). Vitamin C topical formulations are also applied due to their depigmenting activity (6) and antiwrinkle activity through collagen synthesis promotion (7). Despite several cosmeceutical formulations containing vitamin C on the market, very few are topically effective. The major drawbacks in the design of these formulations are: (1) low concentration of vitamin C in the formulations; (2) incomplete absorption and metabolism of different forms of vitamin C (mixture of isomers or ester) by the skin; and (3) chemical instability of vitamin C once the product is opened (3,8). Vitamin C is easily oxidized to dehydroascorbic acid (DHA) due to exposure to air, light, and high temperature, which results in a short shelf time of formulations containing vitamin C (9). The bioactivity of DHA is reported at 80% of the activity of vitamin C (10). In basic conditions, the oxidation of vitamin C occurs rapidly and results in the irreversible hydrolyzation of vitamin C into 2,3-L-diketogulonic acid (2,3-KDG), which is a biologically inactive form (11).

There are several requirements for cosmeceuticals containing vitamin C to be topically effective: 1) They must contain vitamin C in the form of L-ascorbic acid; (2) the concentration of vitamin C must be sufficient enough (~10%); (3) vitamin C must be stable; and (4) the pH of the formulation must be less than the *p*Ka of vitamin C (4.2). The optimum pH of the formulations is ~3.5 (3). In order to attain an effective vitamin C topical formulation with the aforementioned requirements, developing formulations that enhance the stability of vitamin C is required. One way to increase the stability of vitamin C is to chemically modify its structure by esterifying the hydroxyl groups with organic or inorganic long-chain acids (12). Another method is to encapsulate vitamin C within nanoparticles that protect the sensitive bioactive compound from chemical and enzymatic degradation during storage (13).

[1] Department of Chemical Engineering, Waterloo Institute for Nanotechnology, University of Waterloo, 200 University Avenue West, Waterloo, Ontario N2L 3G1, Canada.
[2] CelluForce Inc, 625, Président-Kennedy Avenue, Montreal, Quebec H3A 1 K2, Canada.
[3] To whom correspondence should be addressed. (e-mail: mkctam@uwaterloo.ca)

Recently, there has been an interest in using renewable resources for the design of various novel products. The abundance and biodegradability of natural polymers have led to extensive research in this field. There is an ever-increasing desire to design novel carriers for the delivery of bioactive compounds to increase their stability and improve their properties for enhanced patient compliance. Cellulosic fiber is the most abundant natural material that contains amorphous and crystalline regions. Acid hydrolysis removes the amorphous regions of cellulose yielding individual rigid rod-like crystals called cellulose nanocrystals (CNC). Since the first discovery of CNC in 1949 by Rånby (14), interest in this system has risen due to its availability, high surface area, and aspect ratio. CNC possesses numerous hydroxyl groups that can be further modified with different functionalities (15). CNC is also practically non-toxic, is biocompatible and biodegradable which makes it an excellent candidate for biomedical applications (16). The second most abundant polymer in nature is chitin derived from the shells of marine crustaceans (shrimp and crabs). The partial deacetylation of chitin leads to the production of chitosan (CS). CS is an amino polysaccharide with interesting biological properties such as biocompatibility, biodegradability, antimicrobial, and wound healing properties (17). The protonation of amine groups in acidic media imparts positive charges onto CS allowing the binding of different anionic compounds. CS has a great potential for manipulating the loading and release profiles of bioactive compounds. The antioxidant activity of chitosan and its derivatives has also been studied by researchers over the past several years (18,19). Low-molecular-weight CS, known as CS oligosaccharide (CS_{OS}) is known to have better water solubility and higher antioxidant properties (20,21). Due to the beneficial properties of CNC and CS_{OS} and the numerous advantages of designing novel carrier systems based on abundant natural polymers, we recently reported on the chemical grafting of CS_{OS} onto the surface of CNC via peptidic coupling reaction (22).

There are several studies reported in literature on the applications of CS nanoparticles for the delivery of vitamins (23). Modified CS nanoparticles have been reported as carriers for vitamin C. *N*-Acyl CS modified with different acyl chain lengths has been used to load vitamin C via a sonication method (24). CS nanoparticles have also been prepared by ionic gelation of CS with tripolyphosphate (TPP), which acts as a crosslinking agent. In one study, Jang and coworkers studied the characteristics and stability of vitamin C-loaded CS nanoparticles in aqueous solutions during heat processing. Their results showed an increase in the stability of vitamin C during heat processing and suggested the potential applications of vitamin C-loaded CS nanoparticles as enhanced antioxidants due to the continuous release of vitamin C in food processing (25). CS nanoparticles have also been prepared by similar methods by Alishahi and coworkers to encapsulate vitamin C to increase its stability (26).

In this study, we aim to increase the stability of vitamin C via the formation of complexes between vitamin C and CS_{OS}-grafted CNC via ionic gelation resulting in CNCS/VC complexes. The potential benefits of these complexes in topical applications would be the following: (1) CNC-CS_{OS} particles will both act as a carrier for vitamin C and increase its stability; (2) CNC particles will reduce the oxidation-induced degradation of vitamin C by acting as barriers for oxygen reaching encapsulated vitamin C in the complexes (8); (3) CS has interesting biological properties such as antioxidant, antibacterial, hemostatic, and wound healing properties suitable for topical cosmeceutical applications; (4) CNC-CS_{OS} has high antioxidant activity, pertaining to a dual antioxidant activity of CNCS/VC, i.e., after the release of vitamin C from the complex as a fast and potent antioxidant, the carrier CNC-CS_{OS} also possesses antioxidant properties leading to a synergic and stable antioxidant effect.

EXPERIMENTAL SECTION

Materials

A freeze-dried cellulose nanocrystals (CNC) sample was supplied by FPInnovations and Celluforce Inc.. Chitosan oligosaccharide (average Mn 5,000 Da, DD ~75%) was purchased from Sigma-Aldrich. For TEMPO-mediated oxidation, the following chemicals were purchased from Sigma-Aldrich: TEMPO (98%), sodium hypochlorite (NaOCl) (reagent grade, 10–15% available chlorine) solution, sodium bromide (NaBr) (99.0%), NaOH (1 N) standard solution, HCl (1 N) standard solution, and methanol. For the amide coupling reaction, crosslinkers EDC (1-ethyl-3-(3-dimethylaminopropyl) carbodiimide, commercial grade) and NHS (*N*-hydroxysuccinimide, 98%+) were purchased from Fluka and Acros Organics, respectively. As-received MES (2-(*N*-morpholino) ethanesulfonic acid, >99%), purchased from Sigma, was used as a buffer for the EDC crosslinking reaction. For antioxidant studies, stable free radical 1,1-diphenyl-2-picryl hydrazyl (DPPH) was purchased from Aldrich. Alcohol reagent, consisting of 90% ethanol, 4.6% methanol, and 5.1% isopropyl alcohol, was purchased from Fisher Scientific. Vitamin C (L-ascorbic acid) was obtained from Sigma-Aldrich. For the complexation, acetic acid (>99.7%) and sodium TPP (technical grade 85%) were purchased from Sigma-Aldrich. Millipore de-ionized (D.I.) water was used for all experiments and sample preparations.

Cellulose Nanocrystal–Chitosan Oligosaccharide Synthesis

The synthesis and characterization of CNC-OX and CNC-CS_{OS} were described in detail in our previous paper (22). The surface hydroxyl groups of CNC were oxidized to carboxyl groups using NaClO assisted by 2,2,6,6,-tetramethyl-1-(pyperidinyloxy) radical (TEMPO) (27). Briefly, a homogenous CNC dispersion was prepared by dispersing CNC (1.3 g) in D.I. water (100 mL) followed by 10 min sonication. TEMPO (20 mg) and NaBr (400 mg) were then added to the dispersion after adjusting the pH to 10 using 0.5 M NaOH and stirred for 30 min at room temperature. The oxidation was initiated by slowly adding NaClO 13% (9.8 mL) under gentle agitation while the pH was kept constant at 10, by the continuous addition of 0.5 M NaOH. After approximately 4 h, the reaction was known to be complete when no additional reduction in the pH was observed. The excess oxidant was quenched using methanol (10 mL), and the pH was adjusted to 7 using 0.5 M HCl. The oxidized nanocrystals were dialyzed

using dialysis tube (M_w cut off, 12,000 Da) against distilled water for at least 48 h and freeze-dried. The grafting of CS onto CNC-OX was achieved by a modified method reported by Bulpitt and Aeschlimann (28). CNC-OX (0.2 g, 0.32 mmol COOH) was dissolved in 50 mL D.I. water. A 50 mL solution containing EDC (0.19 g, 1 mmol) and NHS (0.11 g, 1 mmol) was added to the CNC-OX suspension and stirred for 15 min. Another solution containing CS (0.36 g, 1.3 mmol NH2) was dissolved in 100 mL D.I. water and then added to the first solution resulting in a 200 mL reaction volume. MES buffer (1.95 g, 0.05 M) was then added, and the pH was adjusted to 5. The reaction was stirred for 24 h at room temperature and purified using a dialysis tube (M_w cut off, 12,000 Da) against D.I. water for 4 days until the conductivity of the dialysis medium remained constant (29).

Synthesis of CNC-CS_{OS} Vitamin C Complex (CNCS/VC)

To 10 mL 0.1 wt% CNC-CS_{OS} in acetic acid (6*v*/*v*%), 4 mL of freshly prepared vitamin C in D.I. water (1 mg/mL) was added while stirring. After 5 min, 6 mL of sodium TPP (5 mg/mL) was added drop-wise to the solution using a syringe. The pH of the mixture was kept at ~3, while in some experiments the pH was adjusted to ~5. The mixture was then vortexed for 5 min and sonicated for 10 min. Oxygen in the system was removed by bubbling argon into the vessel for 10 min. The vessel was then covered in aluminum foil, and the mixture was left to stir for overnight in darkness.

Transmission Electron Microscopy (TEM)

Transmission electron microscopic (TEM) images of CNC-CS_{OS} and CNCS/VC were recorded using a Philips CM10 TEM with 60 keV acceleration voltages. A few drops of 0.01 wt% aqueous samples were deposited on a carbon-formvar film on 200-mesh copper grids. Excess solvent was removed from the grids placed on top of a filter paper to minimize the agglomeration of particles and the grids were dried over night.

Vitamin C Encapsulation Efficiency and Drug Loading

In order to remove the unbound vitamin C and calculate the encapsulation efficiency and loading of vitamin C, CNCS/VC solution was passed through an ultrafiltration stirred cell (Millipore Corporation, Bedford, USA) with filters having a cut-off pore size of 25 nm (Millipore, VSWP, Ireland). The concentration of free vitamin C in the filtrate was measured at 265 nm using an Agilent 8453 UV-visible spectrophotometer and based on the vitamin C calibration curve. A fresh stock solution containing 100 μg/mL of vitamin C was prepared by dissolving 1.5 mg of vitamin C in 15 mL of D.I. water. The solution was stored in a glass-stoppered bottle, which was covered in an aluminum foil. Standard solutions of different concentrations (50, 25, 18.75, 12.5, 10, 7.5, 5, and 1 μg/mL) were prepared by diluting the stock solution in D.I. water, and the absorbance of these solutions was recorded at wavelength of 265 nm by Agilent 8453 UV-visible spectrophotometer.

The encapsulation efficiency and drug loading were determined indirectly by measuring the free vitamin C in the filtrate using the following expressions:

$$\text{Encapsulation Effieciency}\,(\%) = \frac{[\text{Vitamin C}]_{\text{total}} - [\text{Vitamin C}]_{\text{filtrate}}}{[\text{Vitamin C}]_{\text{total}}} \times 100 \quad (1)$$

$$\text{Drug Loading}\,(\%) = \frac{\text{Weight of Vitamin C loaded}}{\text{Weight of CNCS/VC}} \times 100 \quad (2)$$

Differential Scanning Calorimetry (DSC)

Calorimetric analyses were performed using a Q2000 calorimeter (TA Instruments Inc., USA). Approximately 2 mg of the samples (vitamin C, CNC-CS_{OS}, and CNCS/$VC_{pH=5}$) were placed in standard aluminum pans and sealed by a hermetic aluminum lid. The samples were heated from 20°C to 300°C with a heating rate of 10°C/min under nitrogen atmosphere.

UV-Spectrophotometry for Proving the Complex Formation

Spectra of 0.1 wt% vitamin C, CNC-CS_{OS}, and CNCS/VC in quartz cuvettes (Hellma Analytics) were recorded at a wavelength range of 150 to 350 nm with a scan rate of 600 nm/min using an Agilent 8453 UV-visible spectrophotometer.

Vitamin C *In Vitro* Release Studies

The 2 mL of CNCS/VC complex was placed in a SnakeSkin dialysis tube (Pierce Biotechnology Inc., Mw cut off: 3500 Da) and immersed in 20 mL phosphate buffer saline (PBS, pH=7.4) while being gently stirred in the dark in a closed container at room temperature. At given time intervals, 1-mL aliquots were removed for analysis and replaced with the same volume of fresh release medium to preserve the sink condition. Based on the vitamin C calibration curve, the samples were assayed for vitamin C content. In order to compare the stability of vitamin C loaded in the CNCS/VC complex, a known solution of vitamin C with the same amount of vitamin C loaded in the complexes was placed in a SnakeSkin dialysis tube and immersed in 20 mL PBS buffer as control.

Isothermal Titration Calorimetry (ITC)

The Microcal VP-ITC instrument was used to study the interactions between vitamin C and CNC-CS_{OS} at pH 3 and pH 5. Once the thermal equilibrium was reached, the titrations were performed at a constant temperature by injecting the titrant (vitamin C 100 mM) from a ~282 μL injection syringe into a 1.4551 mL sample cell filled with 0.1 wt% CNC-CS_{OS} solution prepared at the same pH. An injection schedule was automatically performed using an interactive software after setting the number of injections, volume of each injection, and time between each injection. Blank titrations were performed by injecting the same aliquot of vitamin C into water at the same pH to obtain the heat of dilution.

DPPH Radical Scavenging Activity

The antioxidant activity of the samples was measured by a slightly modified DPPH scavenging activity method (30,31). To study the scavenging activity of samples, briefly, 1 mL of test samples at different concentrations were diluted with 1.85 mL alcoholic reagent, and the absorbance was measured as blank. CNC-CS_{OS} samples were prepared in acetic acid (6% *v/v*) to enhance the dispersibility of the nanoparticles. The 150 μL of freshly prepared methanolic solution of DPPH (1 mg/mL) was then added to the solutions. The reaction mixture was shaken well and incubated for 30 min at room temperature in darkness. The absorbance of the resulting solutions was determined at 517 nm against a blank using the Agilent 8453 UV-visible spectrophotometer. Solvents with DPPH were used as control. Each sample was run in triplicate, and the values were averaged. The radical scavenging activity was measured by the reduction in the absorbance of DPPH, and it was calculated using the following equation:

$$\text{DPPH Scavenging Activity}\ (\%) = \frac{A_{\text{Control}} - A_{\text{Sample}}}{A_{\text{Control}}} \times 100 \quad (3)$$

Antioxidant Activity Kinetics

Antioxidant kinetics of CNC samples was studied by measuring the rate constant (k) of each scavenging activity reaction using the same DPPH protocol (32). The 1-mL sample solutions (0.1 wt%) were diluted with 1.85 mL alcoholic reagent, and then 150 μL of freshly prepared methanolic solution of DPPH (1 mg/mL) was added to the solutions. The solution was fully mixed, and the reduction in absorbance was determined at 517 nm at 0 min, and different time intervals over a period of 200 min using Cary 100 Bio UV-visible spectrometer. All experiments were repeated in triplicate. The antioxidant rate constant (k) was calculated using the following equation:

$$-kt = \ln\frac{A_\infty - A_t}{A_\infty - A_0} \quad (4)$$

Where t is time and A_∞, A_t, A_0 are the absorbances at time infinity, time t, and at time zero, respectively.

RESULTS AND DISCUSSION

Synthesis of CNC-CS_{OS} Vitamin C Complex (CNCS/VC)

The structure of CNC-CS_{OS} and vitamin C, along with a schematic representing the mechanism formation of CNCS/VC is shown in Scheme 1. The CNCS/VC complexes were produced spontaneously by the ionotropic gelation between vitamin C, positively charged amino groups on CS_{OS} and TPP (26). Ionotropic gelation is the crosslinking of polyelectrolytes in the presence of counter ions (33). Unlike other crosslinking agents (formaldehyde or gluteraldehyde), TPP is non-toxic (34,35). CS has protonable amine groups, which possess positive charge at pH below 6, and vitamin C possesses many electrophilic groups. Four hydroxyl groups with different acidities are present in vitamin C's structure in positions 2, 3, 5, and 6 giving rise to varying *p*Ka values for each of the hydroxyl group. The strongest acidity belongs to the hydroxyl group in position 3 (*p*Ka=4.2). Hydroxyl groups in position 2 possess a *p*Ka of 11.6. Hydroxyl groups in positions 5 and 6 act as secondary and primary alcoholic residues, respectively (36). CNCS/VC complexes are formed through non-covalent bonds, such as H-bonds and hydrophobic interactions (37). Based on the Lewis acid–base theory, the acidic hydroxyl group in position 3 of vitamin C is expected to react with the amino groups of chitosan (38). At pH 5, additional electrostatic interactions between the amino groups of CS_{OS} in CNC-CS_{OS} and deprotonated hydroxyl groups in vitamin C are expected.

TEM Analyses

The TEM images of CNC-CS_{OS} and CNCS/VC complex are shown in Fig. 1, a and b, respectively. It can be seen that CNCS/VC complexes were larger compared with the loose network structures of CNC-CS_{OS} due to ionic gelation. For TEM studies, two samples were examined, and more than five TEM images were obtained confirming the reproducibility of the images.

Vitamin C Encapsulation Efficiency and Drug Loading

The encapsulation efficiency (EE%) and drug loading (DL%) of vitamin C in CNCS/VC complexes were calculated

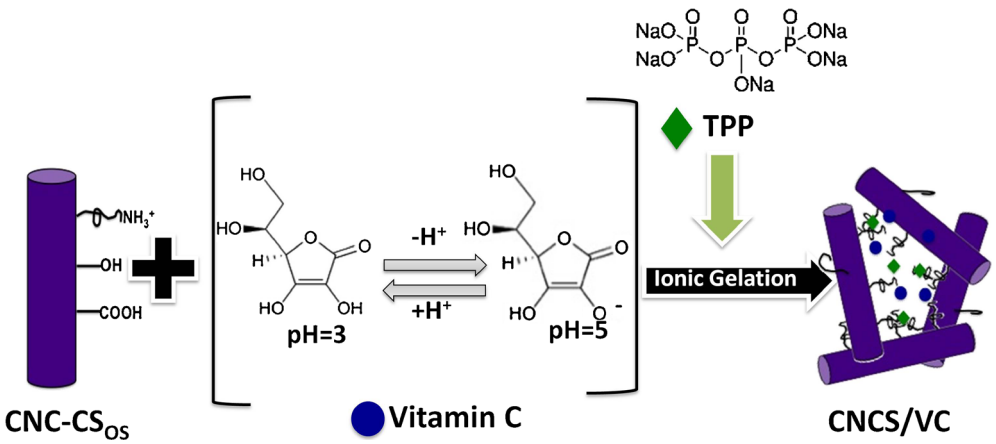

Scheme 1. Schematic illustration of formation of CNCS/VC complex by ionic gelation

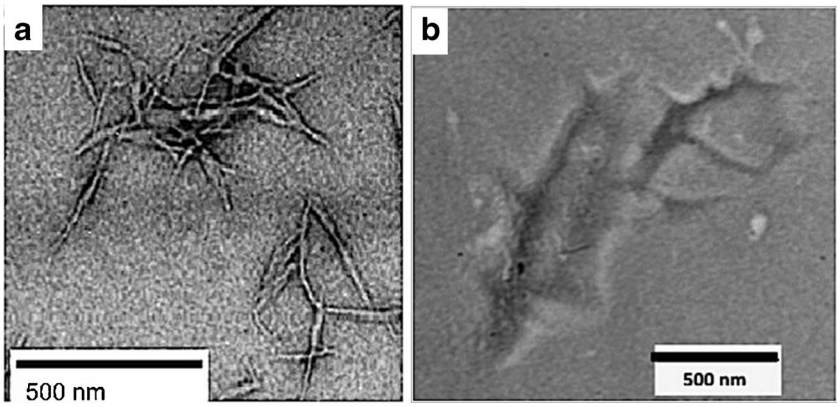

Fig. 1. TEM images of CNC-CS_{OS} and CNCS/VC complex

indirectly by measuring the vitamin C in the filtrate using a vitamin C calibration curve. The results based on three measurements are summarized in Table I. It can be seen that a higher EE% and DL% of vitamin C was observed at pH 5. The first *p*Ka of vitamin C is at pH 4.2. At pH 3, the hydroxyl groups of vitamin C are protonated, and the loading is probably due to physical entrapment of vitamin C and hydrogen bonding with CNC-CS_{OS}. At pH 5, vitamin C is deprotonated, resulting in an additional electrostatic interaction between positively charged CNC-CS_{OS} and the negative charge on vitamin C, leading to a higher encapsulation and loading.

Differential Scanning Calorimetry (DSC)

In order to study the physical state of the materials, DSC analyses of pure vitamin C, CNC-CS_{OS}, and CNCS/VC were performed (Fig. 2). The calorimetric analysis of pure vitamin C displayed a sharp endotherm due to the melting point of vitamin C molecule at 196°C. The absence of the endothermic peak of vitamin C in the CNCS/VC complex indicated the ionic interactions between vitamin C and CNC-CS_{OS} and the complex formation (39). This phenomenon can also be attributed to the miscibility of vitamin C complexed with CNC-CS_{OS} (40).

UV-Spectrophotometry for Proving the Complex Formation

Further confirmation of the insertion of vitamin C in CNC-CS_{OS} was obtained by comparing UV spectra of pure vitamin C, CNC-CS_{OS}, and CNCS/VC (Fig. 3). It can be seen that vitamin C displayed an absorption peak at 265 nm. The CNCS/VC UV spectrum clearly showed the absorption peak of vitamin C, which is indicative of the presence of the vitamin C in its native form. In the presence of amine moieties, the lactone ring in the structure of vitamin C can be subjected to ring opening. The presence of the vitamin C absorption peak in the CNCS/VC complex suggested that vitamin C was not subject to ring opening during the complex formation (38). The shift in the adsorption peak of vitamin C to lower wavelengths in the complex, and its broadening could be attributed to the complexation between vitamin C and reactive groups of CNC-CS_{OS}. Similar results were reported in the literature (41).

Table I. Encapsulation Efficiency (EE%) and Drug Loading (DL%) of vitamin C in CNCS/VC Complexes at pH 3 and pH 5 (n=3)

pH	EE%±SD	DL%±SD
3	71.6±6.8	28.6±2.7
5	91.0±1.0	38.4±2.5

EE encapsulation eficiency, *DL* drug loading, *SD* standard deviation

Vitamin C *In Vitro* Release Studies

The cumulative *in vitro* vitamin C release from CNCS/VC loaded at pH of 3 and 5 is shown in Fig. 4. The *in vitro* release profile of vitamin C loaded at pH 5 showed a more controlled release profile and a higher percentage of vitamin C was released. This could be attributed to the higher loading of vitamin C in the complex at pH 5 which resulted in a higher concentration gradient and faster diffusion. The size of vitamin C is significantly smaller than CNC-CS_{OS}, and the molecules can easily diffuse through the pores and from the surface of the carrier (25). A control solution of vitamin C containing the same amount of vitamin C loaded at pH 3 in CNCS/VC complexes was placed in a dialysis tube and immersed in PBS solution. The control vitamin C solution diffused rapidly from

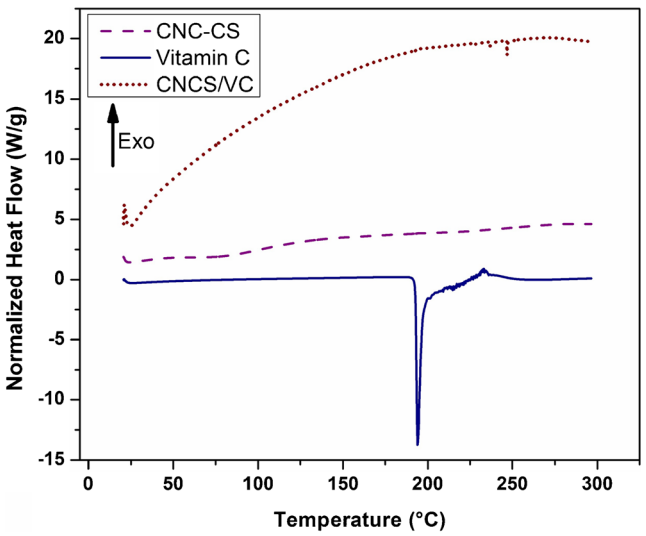

Fig. 2. DSC thermograms of CNC-CSOS, vitamin C, and CNCS/VC complex

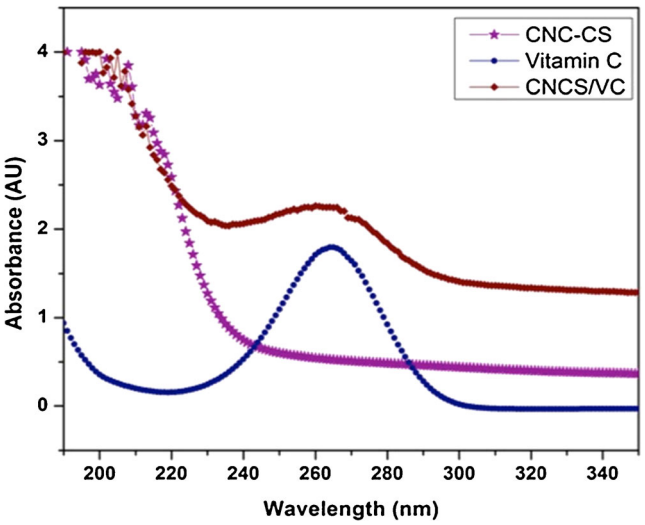

Fig. 3. UV spectrum of CNC-CS_{OS}, vitamin C, and CNCS/VC

the inside the dialysis tube to the release medium and was degraded over time. However, based on Fig. 4, vitamin C loaded in CNCS/VC was released gradually over 20 days from the complex and was more stable. Our results are in accordance with the results reported by Alishahi and coworkers, where they compared the shelf life of free vitamin C with encapsulated vitamin C in CS nanoparticles. Encapsulated vitamin C was more stable whereas a ~70% reduction in free vitamin C concentration was observed over a period of 20 days (42).

Thermodynamics of CNC-CS_{OS} and Vitamin C Interaction

ITC was used to investigate the binding thermodynamics between vitamin C and CNC-CS_{OS} at pH 3 and 5. Figure 5 shows the raw ITC data of titrating 100 mM vitamin C into CNC-CS_{OS} at pH 3 and 5, as well as the blanks containing the same concentration of vitamin C was titrated into water. The

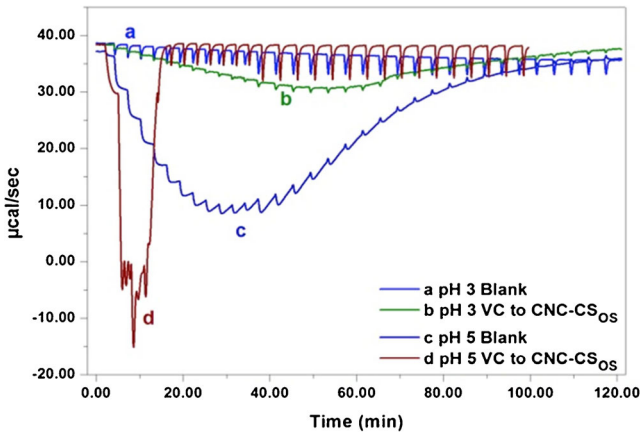

Fig. 5. Raw ITC data for titrating 100 mM vitamin C (VC) into **a** water at pH 3, **b** water at pH 5, **c** CNC-CS_{OS} at pH 5, and **d** CNC-CS_{OS} at pH 3

pH of the titrant and CNC-CS_{OS} solutions were adjusted to the same pH values.

Our results were reproducible and displayed an unusual behavior. At pH 3, titrating vitamin C into water resulted in typical exothermic heat of dilution (plot a). However, when titrating vitamin C into CNC-CS_{OS} at pH 3, we observed small exothermic peaks with a shift in the baseline (plot b). At pH 5, raw ITC plot of titrating vitamin C into water displayed a significant baseline drift with the first titration points being exothermic and the final points being endothermic (plot c). This could be due to the instability of vitamin C at pH 5 leading to a continuous change in the characteristics of the titrant, i.e., vitamin C. Titrating vitamin C into CNC-CS_{OS} at pH 5 resulted in an interesting and reproducible thermogram (plot d). The first few titrations resulted in huge exothermic peaks with a drastic baseline drift. The fact that the equilibrium was not re-established after the first few injections could indicate that the binding of vitamin C to CNC-CS_{OS} at pH 5 was affected by a slow aggregation-like process (43). However, as seen in Fig. 5c, after a fixed number of injections, and once the complex between vitamin C and CNC-CS_{OS} was

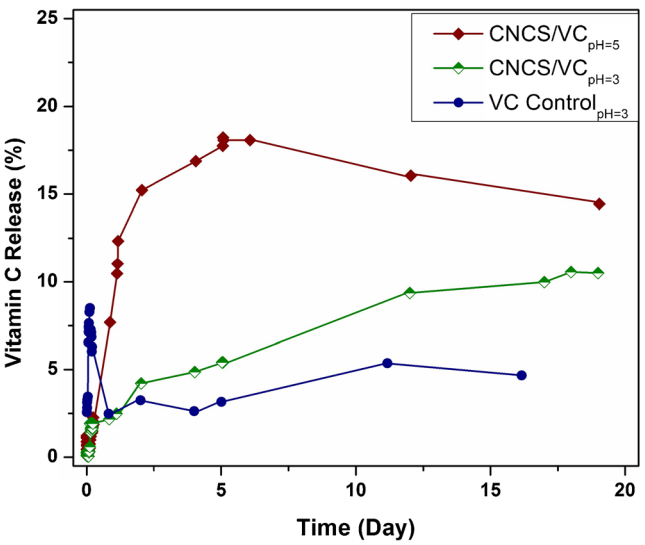

Fig. 4. Vitamin C *in vitro* release profile from CNCS/VC (prepared at pH=5 and pH=3) and control vitamin C (pH=3) in PBS pH=7.4

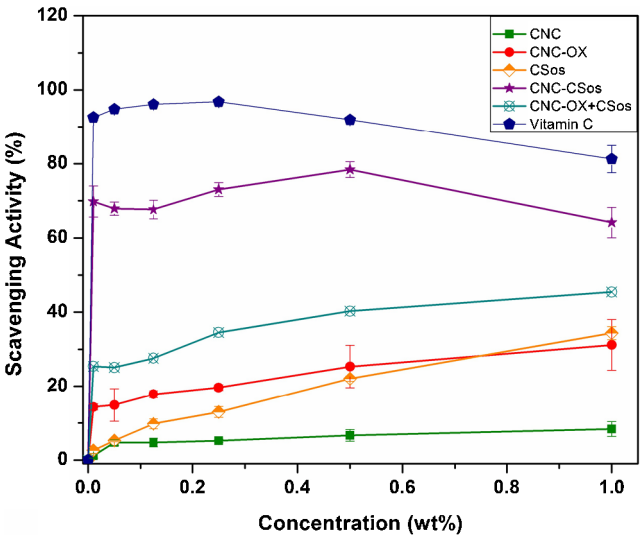

Fig. 6. Scavenging activity of different samples at different concentrations on DPPH radical (n=3)

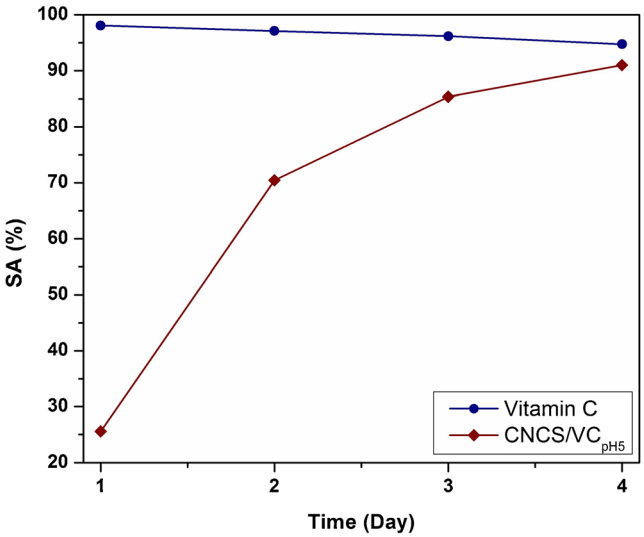

Fig. 7. Scavenging activity of CNCS/VC$_{pH\ 5}$ and vitamin C over time

formed, the equilibrium was re-established after the fifth injection, and there was no drift in the baseline. The huge exothermic peaks when titrating vitamin C into CNC-CS$_{OS}$ at pH 5 compared with pH 3 could be attributed to ionic interactions between negatively charged vitamin C and positively charged CNC-CS$_{OS}$. This result could explain the higher binding efficiency for vitamin C at pH 5 reported in Table I.

DPPH Radical Scavenging Activity

An important antioxidant mechanism involves the scavenging of hydrogen radicals. DPPH possesses a hydrogen radical with a characteristic absorbance of 517 nm. As antioxidants react with DPPH radical, the absorbance at 517 nm decreases, and the purple color of DPPH solution changes to yellow (31). Therefore, by measuring the absorbance using a spectrophotometer, the progress of the reaction can be analyzed (44). In this study, DPPH was used to deduce the antioxidant activity of samples. The scavenging activity (SA%) of the samples on DPPH at various concentrations is shown in Fig. 6. Our results showed that oxidizing the CNC enhanced its antioxidant activity. Also, the SA% of CNC-CS$_{OS}$ was much higher than SA% of the physical mixture of its precursors (CNC-OX+CS$_{OS}$). The scavenging activity of samples depends on their capacity to donate an electron to DPPH. This property is a function of different sizes of electron-cloud density and its accessibility to DPPH (45). The higher SA% of CNC-CS$_{OS}$ compared with its precursors could be due to the orientation of the functional groups of CS chain after chemical conjugation on CNC surface, leading to increased accessibility of the functional groups to react with DPPH radical. The decrease in the SA% of CNC-CS$_{OS}$ at 1 wt% concentration might be attributed to the slight reduction in the solubility of CNC-CS$_{OS}$, leading to a lower antioxidant activity. Moreover, the lower mobility of CNC-CS$_{OS}$ at high concentrations might increase the possibility of inter- and intramolecular bonding that minimized the exposure of active functional groups that were responsible for the scavenging activity.

The SA% of 0.1 wt% CNCS/VC$_{pH5}$ and 0.1 wt% vitamin C was measured in four consecutive days (Fig. 7). It can be seen that the SA% of vitamin C solution slightly decreased over the course of 4 days due to the instability of vitamin C. The SA% of CNCS/VC$_{pH5}$ increased over time as vitamin C was being released from the complex. The results are in accordance with the vitamin C release profile observed in Fig. 4. The low SA% of CNCS/VC$_{pH5}$ on day 1 might be due to the involvement of the functional groups of CNC-CS$_{OS}$ with vitamin C in the complex, preventing the functional groups to react with DPPH radicals.

Antioxidant Kinetics Studies

The antioxidant kinetics of CNC samples was studied by monitoring the decay of the absorbance peak of DPPH at 517 nm over time and calculating the rate constants (k). The antioxidant reaction rate has been proposed as another parameter to elucidate the antioxidant activity of various compounds (46). As seen in Fig. 8, CNC-CS$_{OS}$ possessed the largest slope, leading to the highest rate constant, and the slope of the first-order kinetic plot of CNC-OX was larger than CNC. The high antioxidant rate constant leading to the fastest antioxidant activity observed for CNC-CS$_{OS}$ might be attributed to the presence of several functional

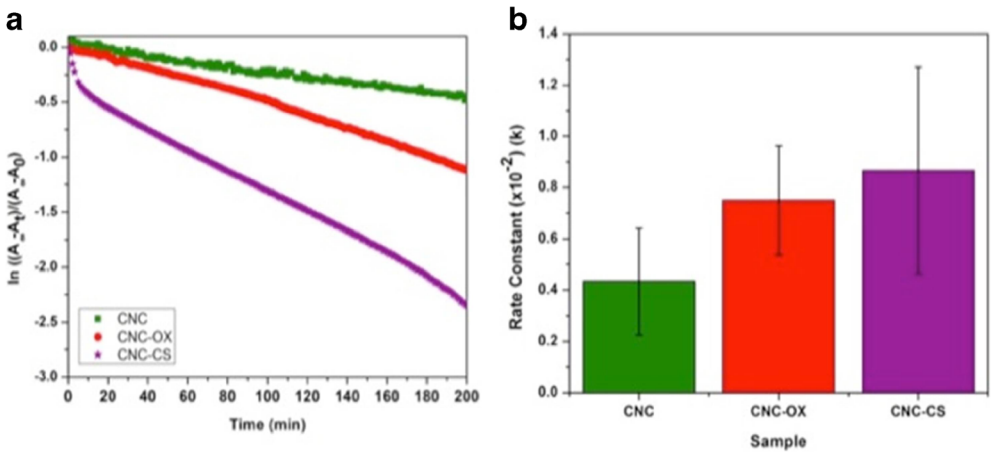

Fig. 8. **a** Decay of the visible absorbance (517 nm) of a DPPH solution following addition of CNC samples. **b** Estimation of antioxidant rate constant for first H atom abstraction (k) for CNC samples using Eq. 4 (n=3)

groups (OH, COOH, and NH_2) on the surface of CNC and their synergistic effect in increasing the speed of the scavenging activity.

CONCLUSIONS

An effective and novel antioxidant system was developed by forming complexes between vitamin C and cellulose nanocrystal grafted chitosan oligosaccharide (CNC-CS_{OS}). CNC-CS_{OS} was first prepared via peptidic coupling by reacting the carboxylic acid groups on oxidized CNC with the amino groups on CS_{OS}. CNCS/VC complexes were then prepared using TPP through ionic complexation of CNC-CS_{OS} and addition of vitamin C at pH 3 and 5. TEM images showed complexes with a size of approximately 1 μm. DSC and UV spectrophotometry confirmed the presence of vitamin C in the CNCS/VC complexes. The encapsulation efficiency of vitamin C was higher (~91%) at pH 5 compared with pH 3 (~72%). The *in vitro* release of vitamin C from CNCS/VC complexes displayed a sustained release up to 3 weeks with the released vitamin C displaying higher stability compared with a control vitamin C solution. DPPH method was used to study the scavenging activity and antioxidant kinetics of various CNC samples, CS_{OS}, and vitamin C as control. CNC-CS_{OS} had higher scavenging activity and antioxidant rate constant compared with oxidized CNC and CS_{OS} and their physical mixture denoting a synergistic activity against DPPH radical. Therefore, by loading vitamin C into CNC-CS_{OS} particles, an efficient dynamic antioxidant agent was produced, and vitamin C is released over time with the carrier CNC-CS_{OS} also possessing desirable antioxidant properties. The pH, high loading, and stability of vitamin C in CNCS/VC complexes make it an excellent candidate for applications in topical cosmeceuticals.

ACKNOWLEDGMENTS

We wish to acknowledge FPInnovations and Celluforce Inc. for providing the cellulose nanocrystals, and the research funding from Celluforce and AboraNano facilitated the research on CNC. We would also like to thank Moin Ahmed and Anthony Wang for their assistance with the antioxidant studies. S. P. Akhlaghi acknowledges César Brinatti for his valuable discussion on ITC. K. C. Tam wishes to acknowledge funding from CFI and NSERC.

REFERENCES

1. Manela-Azulay M, Bagatin E. Cosmeceuticals vitamins. Clin Dermatol. 2009;27:469–74.
2. Darr D, Combs S, Dunston S, Manning T, Pinnell S. Topical vitamin C protects porcine skin from ultraviolet radiation-induced damage. Br J Dermatol. 1992;127:247–53.
3. Burke KE. Interaction of vitamins C and E as better cosmeceuticals. Dermatol Ther. 2007;20:314–21.
4. Pinnell SR, Yang H, Omar M, Riviere NM, Debuys HV, Walker LC, *et al.* Topical L-ascorbic acid : percutaneous absorption studies. Am Soc Dermatol Surg, Inc. 2001;27:137–42.
5. Farris PK. Topical vitamin C. A useful agent for treating photoaging and other dermatologic conditions. Am Soc Dermatol Surg. 2005;31:814–8.
6. Ochiai Y, Kaburagi S, Obayashi K, Ujiie N, Hashimoto S, Okano Y, *et al.* A new lipophilic pro-vitamin C, tetra-isopalmitoyl ascorbic acid (VC-IP), prevents UV-induced skin pigmentation through its anti-oxidative properties. J Dermatol Sci. 2006;44:37–44.
7. Murad S, Grove D, Lindberg KA, Reynolds G, Sivarajah A, Pinnell SR. Regulation of collagen synthesis by ascorbic acid biochemistry. Proc Natl Acad Sci USA. 1981;78:2879–82.
8. Piao H, Kamiya N, Cui F, Goto M. Preparation of a solid-in-oil nanosuspension containing L-ascorbic acid as a novel long-term stable topical formulation. Int J Pharm. 2011;420:156–60.
9. Davey MW, Van Montagu M, Inze D, Sanmartin M, Kanellis A, Smirnoff N, *et al.* Review plant L-ascorbic acid : chemistry, function, metabolism, bioavailability and effects of processing. J Sci Food Agric. 2000;860:825–60.
10. Ogiri Y, Sun F, Hayami S, Fujimura A, Yahahoto K, Yaita M, *et al.* Very low vitamin C activity of orally administered L-dehydroascorbic acid. J Agric Food Chem. 2002;50:227–9.
11. Simpson GLW, Ortwerth BJ. The non-oxidative degradation of ascorbic acid at physiological conditions. Biochim Biophys Acta. 2000;1501:12–24.
12. Idson B. Vitamins and the skin. Cosmet Toilet. 1993;108:79–94.
13. Mao HQ, Roy K, Troung-Le VL, Janes KA, Lin KY, Wang Y, *et al.* Chitosan-DNA nanoparticles as gene carriers: synthesis, characterization and transfection efficiency. J Control Release. 2001;70:399–421.
14. Rånby G. Fibrous macromolecular systems cellulose and muscle, the colloidal properties of cellulose micelles. Discuss Farday Soc. 1951;IV:158–64.
15. Azizi Samir MAS, Alloin F, Dufresne A. Review of recent research into cellulosic whiskers, their properties and their application in nanocomposite field. Biomacromolecules. 2005;6:612–26.
16. De Souza Lima MM, Borsali R. Rodlike cellulose microcrystals: structure, properties, and applications. Macromol Rapid Commun. 2004;25:771–87.
17. Sonia TA, Sharma CP. Chitosan and its derivatives for drug delivery perspective. Advanced polymer sciences. Berlin Heidelberg: Springer-Verlag; 2011. p. p. 23–54.
18. Xie W, Xu P, Liu Q. Antioxidant activity of water-soluble chitosan derivatives. Bioorg Med Lett. 2001;11:1699–701.
19. Yen M-T, Yang J-H, Mau J-L. Antioxidant properties of chitosan from crab shells. Carbohydr Polym. 2008;74:840–4.
20. Chae SY, Son S, Lee M, Jang M-K, Nah J-W. Deoxycholic acid-conjugated chitosan oligosaccharide nanoparticles for efficient gene carrier. J Control Release. 2005;109:330–44.
21. Xing R, Liu S, Guo Z, Yu H, Wang P, Li C, *et al.* Relevance of molecular weight of chitosan and its derivatives and their antioxidant activities in vitro. Bioorg Med Chem. 2005;13:1573–7.
22. Akhlaghi SP, Berry RC, Tam KC. Surface modification of cellulose nanocrystal with chitosan oligosaccharide for drug delivery applications. Cellulose. 2013;20:1747–64.
23. Janes KA, Calvo P, Alonso MJ. Polysaccharide colloidal particles as delivery systems for macromolecules. Adv Drug Deliv Rev. 2001;47:83–97.
24. Cho Y, Kim JT, Park HJ. Size-controlled self-aggregated *N*-acyl chitosan nanoparticles as a vitamin C carrier. Carbohydr Polym. 2012;88:1087–92.
25. Jang II K, Lee HG. Stability of chitosan nanoparticles for L-ascorbic acid during heat treatment in aqueous solution. J Agric Food Chem. 2008;56:1936–41.
26. Alishahi A, Mirvaghefi A, Tehrani MR, Farahmand H, Koshio S, Dorkoosh FA, *et al.* Chitosan nanoparticle to carry vitamin C through the gastrointestinal tract and induce the non-specific immunity system of rainbow trout (*Oncorhynchus mykiss*). Carbohydr Polym. 2011;86:142–6.
27. Saito T, Isogai A. TEMPO-mediated oxidation of native cellulose. The effect of oxidation conditions on chemical and crystal structures of the water-insoluble fractions. Biomacromolecules. 2004;5:1983–9.
28. Bulpitt P, Aeschlimann D. New strategy for chemical modification of hyaluronic acid: preparation of functionalized derivatives and their use in the formation of novel biocompatible hydrogels. J Biomed Mater Res [Internet]. 1999;47(2):152–69.
29. Azzam F, Heux L, Putaux J-L, Jean B. Preparation by grafting onto, characterization, and properties of thermally responsive

polymer-decorated cellulose nanocrystals. Biomacromolecules. 2010;11:3652–9.
30. Shimada K, Fujikawa K, Yahara K, Nakamurat T. Antioxidative properties of xanthan. J Agric Food Chem. 1992;40:945–8.
31. Brand-Williams W, Cuvelier ME, Berset C. Use of a free radical method to evaluate antioxidant activity. Leb Wiss U Technol. 1995;30:25–30.
32. Tam J, Liu J, Yao Z. Effect of microstructure on the antioxidant properties of fullerene polymer solutions. RSC Adv. 2013;3:4622–7.
33. Patil P, Chavanke D, Wagh M. A review on ionotropic gelation method: novel approach for controlled gastroretentive gelispheres. Int J Pharm Pharm Sci. 2012;4:27–32.
34. Lim LY, Wan LSC, Thai PY. Chitosan microspheres prepared by emulsification and ionotropic gelation. Drug Dev Ind Pharm. 1997;23:981–5.
35. Desai KGH, Park HJ. Encapsulation of vitamin C in tripolyphosphate cross-linked chitosan microspheres by spray drying. J Microencapsul. 2005;22:179–92.
36. Capuzzi G, Nostro PL, Kulkarni K, Fernandez JE. Mixtures of stearoyl-6-*O*-ascorbic acid and r-tocopherol : a monolayer study at the gas/water interface. Langmuir. 1996;12:3957–63.
37. Dikusar EA, Kozlov NG, Melnichuk LA. Salts of L-ascorbic acid with certain substituted amines and triphenylphosphine. Chem Nat Compd. 2004;40:406–7.
38. Tian XL, Tian DF, Wang ZY, Mo FK. Synthesis and evaluation of chitosan–vitamin C complex. Indian J Pharm Sci. 2009;71:371–6.
39. Xiaolin T, Dafeng T, Zhongyan W, Fengkui M. Synthesis and evaluation of chitosan–vitamin C complexes. J Appl Polym Sci. 2009;114:2986–91.
40. Park S-I, Zhao Y. Incorporation of a high concentration of mineral or vitamin into chitosan-based films. J Agric Food Chem. 2004;52:1933–9.
41. Curcio M, Puoci F, Iemma F, Parisi OI, Cirillo G, Spizzirri UG, *et al*. Covalent insertion of antioxidant molecules on chitosan by a free radical grafting procedure. J Agric Food Chem. 2009;57:5933–8.
42. Alishahi A, Mirvaghefi A, Tehrani MR, Farahmand H, Shojaosadati SA, Dorkoosh FA, *et al*. Shelf life and delivery enhancement of vitamin C using chitosan nanoparticles. Food Chem. 2011;126:935–40.
43. Kasimova MR. On the temperature dependence of complex formation between chitosan and proteins. Biomacromolecules. 2011;12:2534–43.
44. Molyneux P. The use of the stable free radical diphenylpicrylhydrazyl (DPPH) for estimating antioxidant activity. Songklanakarin J Sci Technol. 2004;26:211–9.
45. Chen SK, Tsai ML, Huang JR, Chen RH. In vitro antioxidant activities of low-molecular-weight polysaccharides with various functional groups. Agric Food Chem. 2009;57:2699–704.
46. Sanchez-Moreno C. Review: methods used to evaluate the free radical scavenging activity in foods and biological systems. Food Sci Technol Int. 2002;8:121–37.